Annals of Nuclear Medicine Vol. 19, No. 2, 75–82, 2005

Characterization of ordered-subsets expectation maximization with 3D post-reconstruction Gauss filtering and comparison with filtered backprojection in ^{99m}Tc SPECT

Marco Brambilla,* Barbara Cannillo,* Marco Dominietto,*
Lucia Leva,** Chiara Secco* and Eugenio Inglese**

*Health Physics Department, **Nuclear Medicine Department,
Azienda Ospedaliera "Maggiore della Carità," Novara, Italy

Purpose: To characterize ordered-subset expectation maximization algorithm with a fixed 3D Gauss post-reconstruction filtering (OSEM) in ^{99m}Tc SPECT as for noise, contrast and spatial resolution with varying number of subset and iteration and to compare OSEM with an optimized set of parameters, with filtered backprojection (FBP) with filter parameters typical of brain and myocardial SPECT, both with and without Chang's method of attenuation correction (AC). ***Methods:*** SPECT images of a Jaszczak phantom with cold rod inserts, hot and cold spheres and capillary line sources were acquired. Different background activity concentrations of the phantom were simulated as well as different lesion-to-background activity ratios. OSEM reconstructions were halted after 5, 10 and 15 iterations using 4, 8 and 16 subsets. ***Results:*** The effect of subset and iteration number over noise is additive: thus, it is possible to define an EM-equivalent iteration number that indicates the product between the subset and the iteration numbers. Noise increases linearly with increasing EM-equivalent iteration number. For each level of nominal contrast, the measured contrast after OSEM shows a little increase with increasing iteration number and saturates after 80 EM-equivalent iterations. The application of AC leads to diminished contrast values both in FBP and OSEM. The contrast of cold lesions after OSEM increases with increasing number of EM-equivalent iteration number: after 80 iterations the contrast values with OSEM overtake the ones obtained with FBP; contrast values diminished as background concentration raised. Resolution values did not change with increasing EM-equivalent iteration number and were higher than those obtained with FBP. ***Conclusion:*** The major findings of the present work are the demonstration of additivity of subset and iteration in OSEM over noise, with the possibility of defining an EM equivalent iteration number, and the superiority of OSEM with respect to FBP in terms of spatial resolution.

Key words: iterative reconstruction, ordered-subsets expectation maximization, filtered backprojection, SPECT

INTRODUCTION

Iterative reconstruction algorithms are finding widespread use in commercial software because of increase in computer power and are becoming a clinically practical alternative to filtered backprojection (FBP). Maximum-likelihood expectation maximization (MLEM) algorithm has been widely investigated, so that its noise and convergence properties are well known.[1–4] In particular MLEM has improved noise properties over FBP and eliminates streaking artifacts, which are common in noisy FBP studies. Unfortunately, convergence requires too many iterations to be practical for use in clinical routine.[3]

Ordered-subset expectation maximization (OSEM) algorithm,[5] which is related to but much faster than

Received July 12, 2004, revision accepted October 25, 2004.

For reprint contact: Marco Brambilla, M.D., Servizio di Fisica Sanitaria, A.O. "Maggiore della Carità", C.so Mazzini 18–28100 Novara, ITALY.

E-mail: marco.brambilla@maggioreosp.novara.it

MLEM, has become the dominant iterative reconstruction procedure in SPECT. Both MLEM and OSEM have the ability to model Poisson noise and the exact photon transport. Even scatter and distance dependent camera response can be modeled in detail resulting in truly quantitative images and in better noise contrast tradeoff.[6–10] Nevertheless, as pointed out by Lalush et al.[11] to date the only way to prove that these algorithms are accurate and effective is through careful empiric studies.

The performances of OSEM and FBP have been compared in a number of experimental and clinical studies[12–16] with a variety of reconstruction parameters employed with OSEM, including number of subset, number of iteration and the type and amount of post-reconstruction smoothing to reduce noise with increasing number of iterations: Blocklet et al.[12] compared FBP and OSEM (8 subsets and 2 iterations without post filtering) in bone SPECT reconstruction; Case et al.[13] compared attenuation correction techniques in bone SPECT of the spine using OSEM (12 subsets and 3 iterations, 3D Wiener filter); Kauppinen et al.[14] compared FBP and OSEM (6 subsets and 4–12 iterations, Butterworth post filtering) in brain perfusion SPECT with scatter and non uniform attenuation correction; Vanhove et al.[15] implemented OSEM algorithm for data acquired with a pinhole collimator in phantom studies: using OSEM different iterations were used in combination with 1–32 subsets. Wells et al.[16] compared FBP and OSEM (8 subsets and 1 iteration, 3D Gauss) for small-lesion detection and localization in ^{67}Ga SPECT.

The choice of which parameters to employ in OSEM algorithm during image reconstruction is not entirely obvious. The problem is intrinsically multifactorial: OSEM results depend not only on subset and iteration number but also on pixel size and amount of post reconstruction filtering. According to OSEM theory, in noiseless situation the effect of subset and iteration number should be additive over noise. It has to be demonstrated that the same holds true in noisy situations. In the present work OSEM performances were characterized with respect to subset and iteration number, having fixed the pixel size and the amount of post reconstruction filtering. OSEM performances were expressed in terms of noise, resolution and contrast in simulated hot and cold lesions.

The OSEM algorithm in ^{99m}Tc SPECT with an optimized set of parameters, was compared with filtered backprojection (FBP) with filter parameters typical of brain and myocardial SPECT studies, both with and without Chang's method of attenuation correction (AC).

MATERIALS AND METHODS

Phantom study

The phantom used was a Jaszczak phantom (Deluxe ECT Data Spectrum Corporation, Chapel Hill, USA), depicted in Figure 1. The phantom was a standardized diameter cylinder with an assortment of inserts. The inserts included six solid and six void spheres (diameters: 9.5, 12.7, 15.9, 19.1, 25.4, 31.8 mm), a cold rod insert (diameters: 4.8, 6.4, 7.9, 9.5, 11.1, 12.7 mm) and capillary line sources (inner diameter: < 1 mm). In order to simulate different background activity concentrations the phantom was filled with uniform ^{99m}Tc solution of 37 kBq/m*l* and 12.3 kBq/m*l*, hereafter referred as high and low background. To introduce some variability, 5 hot lesions were created (filling the void spheres) with lesion-to-background activity ratios of 2:1, 5:1, 8:1 and 3:1, 30:1 in the case of high and low background activity concentration, respectively. Hereafter, they will be referred to as nominal contrast C_{nom}, where C_{nom} = 29 [(30 – 1)/1] and 2 [(3 – 1)/1] represent the low background activity , while C_{nom} = 7, 4 and 1 (following the same notation) represent the high background activity. It must be acknowledged that there are relative uncertainties in these assays, which we believe are on the order of ±5%. The hot sphere contrast ratio depends on the relative accuracy of these assays and thus will exhibit corresponding uncertainties on the order of ±10%.

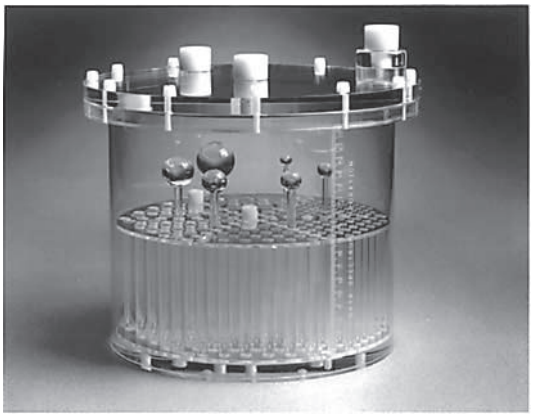

Fig. 1 Jaszczak phantom with cold rod inserts, hot and cold spheres.

SPECT imaging

Image acquisition was performed with a Siemens E-Cam dual-head scintillation camera equipped with a low energy high resolution collimator (Siemens Medical Systems, Inc., Hoffman Estates, Ill., USA). SPECT acquisitions were performed using a 180° non circular orbit for each detector, with 128 projection angles, 128 × 128 matrix size, zoom = 1 and pixel size of 4.75 mm. A symmetrical 15% wide energy window for the acquisition was centered at 140 keV. The phantom studies were acquired for 30 sec per projection angle. A total of 8 tomographic acquisitions were performed: 5 with hot sphere inserts with different lesion-to-background activity ratios and background activity; 2 with cold sphere inserts and different background activity; 1 with capillary line sources imbedded in water to assess tomographic

resolution with scatter. Acquisitions were taken within two hours of phantom preparation.

Image processing

The scintillation camera was connected to a Siemens E-Soft acquisition and processing computer (Siemens Medical Systems, Inc., Hoffman Estates, Ill., USA). The reconstruction algorithms considered in this study were FBP and OSEM. The images reconstructed with FBP were pre filtered with 2 dimensional Butterworth filter[17] of order 5 and a cutoff of 0.7 and 0.5 Nyquist (0.74 and 0.53 cycles/cm) in the case of high and low count density of images. The first choice is typical of brain studies[14] while the second is typical of that used in clinical ^{99m}Tc-sestamibi myocardial SPECT studies.[18–20] The standard first-order Chang attenuation correction[21] was applied to reconstructed slices. Briefly, an attenuation map, based on patient (or phantom) boundary determination and an approximate constant linear attenuation coefficient of the medium μ, is generated and applied to the reconstruction transverse slice. This method will only work well when μ is, in fact, approximately constant (e.g. brain or abdomen). The linear attenuation correction was set to $\mu = 0.11$ cm^{-1}.

Iterative reconstruction program OSEM (Siemens Medical Systems, Inc., Hoffman Estates, Ill., USA) installed in the E-Soft system was used for iterative reconstruction. The images reconstructed with OSEM were filtered with a symmetric 3-D Gaussian function[22] having a full width at half maximum of 1 pixel (4.75 mm). Iterative reconstruction of these images was halted after 5, 10 and 15 iterations using 4, 8 and 16 subsets. Each combination of subsets and iterations was applied to the same set of noisy projection data.

Data analysis

Data were analyzed according to the guidelines for the quality controls of SPECT systems, elaborated by the Italian Association of Nuclear Medicine,[23] as follows:

Noise: One transverse slice was reconstructed through the center of the uniform portion of the phantom using reconstruction techniques detailed in Table 1. Two additional transverse slices were also reconstructed and centered about ± 20 mm from the center along the axis of rotation. Quantitative noise assessment was obtained from slices having at least 2×10^6 counts statistics. A circular region of interest of 50 mm diameter was positioned in the center of the slice. Noise was assessed as percentage root mean square % rms = $100 \times \sigma/M$, being M and σ the mean and the standard deviation of pixel counts in the region of interest.

Contrast: For each lesion in a single reconstructed slice, the signal S was defined as the average pixel value in a region of interest, centered over the lesion and with a diameter of about half the lesion diameter. For the 10 mm diameter lesion, a ROI of two pixels covering the entire area of the lesion was employed. The background B was defined as the average pixel value in a circular ROI (diameter = 50 mm) positioned in the uniform region of the phantom.

Contrast C was defined as:

$$C = \frac{|B - S|}{B}$$

Quantitative assessment of contrast was obtained from slices having at least 2×10^6 counts statistics. Measured contrast values were plotted as the percentage of the nominal contrast value versus EM-equivalent iteration number and versus lesion diameter, with and without AC.

Spatial resolution with scatter: One transverse slice, 2 pixels in thickness, was reconstructed through the center of the phantom using reconstruction techniques detailed in Table 1. Two additional transverse slices of the same thickness were also reconstructed and centered about ±20 mm from the center along the axis of rotation. The three reconstructed points in each of the three reconstructed slices were analyzed individually with a square region of interest. Each region of interest was centered on the maximum count pixel. The size of the square region of interest was at least four times the anticipated FWHM of the count profile to be analyzed. For each point in the images, the FWHM in X and Y was determined. The average FWHM radial value of the six radial measurements on the three slice images of the two peripheral sources was calculated. Likewise, the average tangential FWHM value of the six tangential measurements on the images of the two peripheral sources was calculated. Also the average of the six measurements (three in the X direction and three in the Y direction) for the three images of the center source was calculated. Measured resolution values were plotted as FWHM (mm) values versus iteration number.

Table 1 ANOVA table for the factorial model referring to the influence of subset and iteration number on % rms noise. Background activity concentration = 37 kBq/m*l*

Source of variation	Degrees of freedom	Sum of squares	Mean square	Variance ratio (F)	P value
Subset (A)	2	187.53	93.76	37.46	< 0.0001
Iteration (B)	2	108.42	54.21	21.67	< 0.0001
AB	4	8.46	2.11	0.85	0.515
Error	18	45.06	2.50		

Table 2 ANOVA table for the factorial model referring to the influence of subset and iteration number on % rms noise. Background activity concentration = 12.3 kBq/m*l*

Source of variation	Degrees of freedom	Sum of squares	Mean square	Variance ratio (F)	P value
Subset (A)	2	108.88	54.44	82.00	< 0.0001
Iteration (B)	2	57.23	28.62	43.11	< 0.0001
AB	4	10.21	2.55	3.96	0.043
Error	9	5.98	0.64		

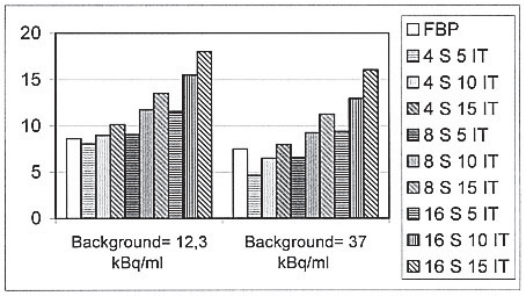

Fig. 2 Noise (% rms) with varying number of subset and iteration in OSEM. S = subset number; IT = iteration number.

Statistical analysis

Continuous variables were expressed as mean and standard deviation.

Noise analysis in iterative reconstruction with varying numbers of subsets and iterations was performed by means of a two factor factorial ANOVA, non repeated measures, balanced model.[24] The factorial model allows the simultaneous assessment of the influence of factors over the dependent variable, also keeping into account the interaction between factors. The two factors were subsets (three levels of 4, 8, 16 subsets) and iterations (three levels of 5, 10, 15 iterations). The dependent variable was noise. There were two and three identical experimental phantom data with low and high background concentration, respectively.

The influence of different reconstruction strategies (OSEM, OSEM with AC, FBP, FBP with AC) over "hot" lesion contrast was assessed by single factor repeated measures ANOVA for each level of lesion-to-background activity ratios. The statistical significance of differences in contrast between different methods of reconstruction was assessed by Fisher's protected least significant difference (PLSD) method. Statistical significance was set at $p = 0.01$.

RESULTS

Noise increases with increasing number of subsets and iteration, as shown in Figure 2. This increase is statistically significant ($p < 10^{-4}$). No significant interaction was evidenced between subsets and iterations ($p = 0.04$ and $p = 0.53$ for low and high background). That is, the effect of subset and iteration number over noise is additive. In

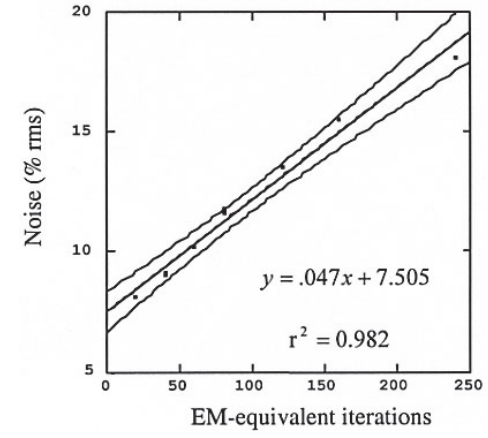

Fig. 3 a: Linear regression with 95% confidence intervals between % rms noise and EM-equivalent iteration number, in a low background activity concentration. b: Linear regression with 95% confidence intervals between % rms noise and EM-equivalent iteration number, in a high background activity concentration.

Table 1 and 2 are reported ANOVA tables for the two factor factorial model referring to the influence of subset and iteration number on % rms noise, with low and high background.

Since no interaction is present, the EM-equivalent iteration number may be considered as the independent variable in a linear regression study, being the % rms noise the dependent variable. The regression lines together with r^2 correlation coefficients are shown in Figures 3a and 3b

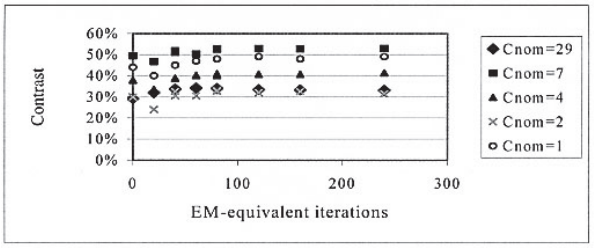

Fig. 4 The measured contrast in a hot lesion of 19.1 mm diameter, for different C_{nom}, versus EM-equivalent iteration number. FBP values correspond to iteration zero.

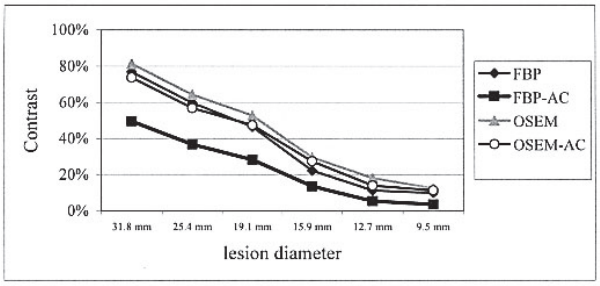

Fig. 5 Measured contrast in hot lesion with C_{nom} = 7 versus lesion diameters, with four different reconstruction strategies (OSEM: 8 subset; 10 iteration; FBP: Butterworth order 5; Fc = 0.7 Nyquist).

Table 3 Post-hoc comparison among reconstruction methods means of measured contrast values for different C_{nom}

Comparison	C_{nom} = 29	C_{nom} = 7	C_{nom} = 4	C_{nom} = 2	C_{nom} = 1
FBP vs. FBP-AC	1.9	14.9*	4.6	6.2*	13.0*
FBP vs. OSEM	–6.3*	–5.3	–8.0*	–9*	–6.0*
FBP vs. OSEM-AC	–6.1*	–0.7	–2.1	–0.3	8.3*
FBP-AC vs. OSEM	–8.2*	–20.2*	–12.7*	–15.2*	–19*
FBP-AC vs. OSEM-AC	–7.9*	–15.6*	–6.6*	–6.5*	–4.7
OSEM vs. OSEM-AC	0.3	4.6	5.9*	8.7*	14.3*
Fisher PLSD	3.3	7.5	4.8	3.0	6.0

*Statistically significant differences

for low and high background, respectively. The slope of the two regression lines is nearly identical (0.047 vs. 0.050), while the noise at zero iterations is different (7.5% vs. 4.7%) for low and high background. The correlation is almost perfect with high r^2 values.

In Figure 4 measured contrast in a "hot" lesion of 19.1 mm diameter, expressed as a percentage of C_{nom}, is reported for different levels of C_{nom} and with respect to the EM-equivalent iteration number. Corresponding to a zero abscissa is reported the contrast measured with FBP. For each level of C_{nom}, the measured contrast after OSEM shows a little increase with increasing number of iterations. Contrast enhancement stops after 80 EM-equivalent iteration, approximately. A further increase in iterations brings no additional gain in contrast. At this level of EM-equivalent iteration number, the maximum gain in contrast (16.4%) between OSEM and FBP is obtained for C_{nom} = 29. There is no clear dependence of contrast from C_{nom}.

In Figure 5 measured contrast for each lesion diameter (with C_{nom} = 7) is reported with four reconstruction strategies: FBP, FBP with AC, OSEM and OSEM with AC. The numbers of subsets and iterations in OSEM were fixed at 8 and 10, respectively (in the region of contrast saturation). A similar trend was observed when the remaining C_{nom} were examined.

The minimum lesion diameter visually detectable was independent of the reconstruction method but dependent on C_{nom}, as expected: lesions with a diameter of 9.5 mm or less were detectable with $C_{nom} \geq 8$; only lesions with a diameter ≥ 12.7 mm were detectable with $5 \leq C_{nom} < 8$; only lesions with a diameter ≥ 19.1 mm were detectable with $2 \leq C_{nom} < 5$.

Repeated measures ANOVA analysis demonstrated the presence of significant differences ($p < 10^{-4}$) among reconstruction methods with respect to measured contrast values, for each level of C_{nom}. Post-hoc comparisons between reconstruction method are provided in Table 3, for each level of C_{nom}. For each treatment comparison the following information is provided: difference between the contrast means and Fisher's PLSD test. If the Fisher's test is significant an asterisk appears by the comparison value. Table 3 indicates that the application of Chang's attenuation correction leads to diminished contrast values both in FBP and OSEM. The smaller values of contrast are obtained with FBP-AC, intermediate values are obtained with FBP and OSEM-AC; highest values are obtained with OSEM. It is worth noting that for some level of C_{nom}, statistical significance might not be attained due to the small statistical power of the tests, due in turn to the small sample size.

In Figure 6 the measured contrast in a "cold" lesion of 19.1 mm diameter, expressed as a percentage of nominal contrast, is reported for two different levels of background activity concentration and with respect to the EM-equivalent iteration number. Corresponding to a zero

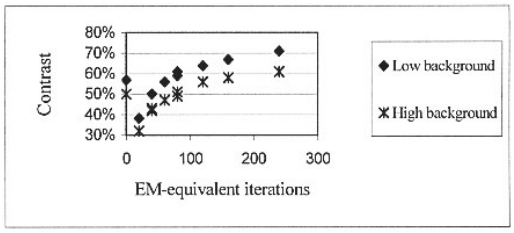

Fig. 6 Measured contrast in a cold lesion of 19.1 mm diameter versus EM-equivalent iteration number. FBP values correspond to iteration zero.

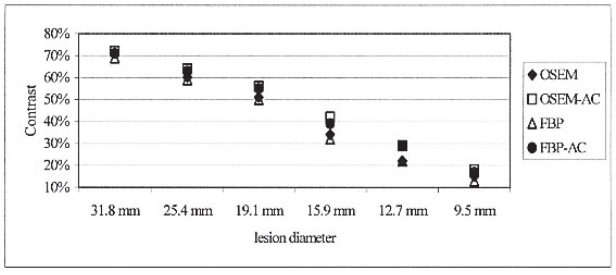

Fig. 7 Measured contrast in cold lesions with a high background activity concentration versus lesion diameters, with four different reconstruction strategies (OSEM: 8 subset; 10 iteration; FBP: Butterworth order 5; Fc = 0.7 Nyquist).

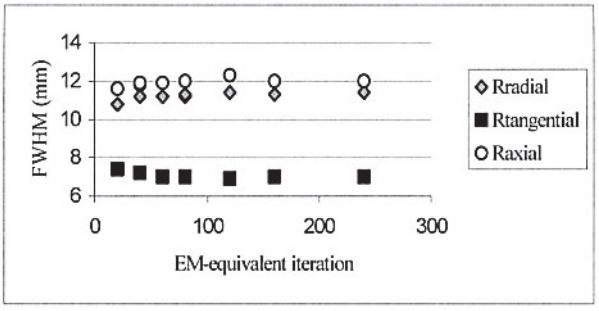

a

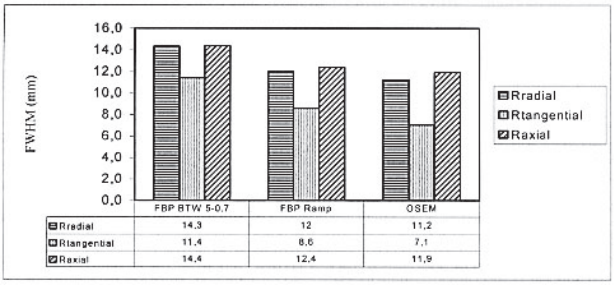

b

Fig. 8 a: Spatial resolution with scatter versus EM-equivalent iteration number. b: Spatial resolution with scatter in OSEM and FBP with ramp filter and Butterworth (order 5, cutoff 0.7 Nyquist) filter.

abscissa is reported the contrast measured with FBP. For each level of background, the measured contrast after OSEM shows an increase with increasing EM-equivalent iteration number. Approximately after 80 iterations the contrast values with OSEM surpass the corresponding values obtained with FBP. Contrast values diminish as background concentration increases.

In Figure 7 measured contrast for high background concentration was reported with four reconstruction strategies: FBP, FBP with AC, OSEM and OSEM with AC. The numbers of subsets and iterations in OSEM were fixed at 8 and 10. These figures indicate that contrast values overlap with FBP and OSEM and the application of AC leads to a slight increase in contrast both with FBP and OSEM. A similar trend was observed for low background concentration.

In Figure 8a the tomographic spatial resolution with scatter, expressed as axial, radial and tangential FWHM in mm, is reported with respect to the EM-equivalent iteration number. Resolution values did not change with increasing number of subsets and iterations. In Figure 8b the values of spatial resolution obtained with OSEM are compared with the values obtained with FBP, with a ramp filter and with a high resolution filter used in clinical practice.

DISCUSSION

In this work OSEM performances were characterized with respect to subset and iteration number, having fixed the pixel size and the amount of post reconstruction filtering. The pixel size was set according to the one used in our laboratory for brain studies. The type of post reconstruction filtering (Gaussian 3D) is the only available choice in the software employed. The FWHM of 1 pixel was chosen on the basis of qualitative judgments performed over clinical images reconstructed both with OSEM and FBP, as the one that provided images of comparable texture and quality with respect to conventional FBP.

In studies reconstructed using EM, in the absence of regularization, as iteration number increases, noise increases.[25] The same is true for studies reconstructed with OSEM and a fixed amount of 3D post-reconstruction Gauss filtering. According to OSEM theory, in the noiseless situation the effect of subset and iteration number should be additive over noise (e.g. 8 subsets and 10 iterations produce the same amount of noise as 5 subset and 16 iterations). The present study demonstrated that the same is true also with noise and different background levels.

The linear relationship between noise and subset times iteration number leads to a predictable (at least in the range explored) and accurate characterization of this increase: % rms increases at a rate of 1% every 20 iterations approximately, both with low and high activity background. Noise equivalence between FBP and OSEM is reached at 23 and 55 iterations with low and high background. Above these thresholds noise is higher in OSEM

than in FBP.

Sphere contrast in simulated "hot" lesions saturates after about 80 iterations in OSEM reconstruction. The finding of contrast saturation at increasing number of iterations after Gaussian regularization was previously reported by Wallis et al.[26] for ML and a number of iterative-weighted methods with and without attenuation correction. This is a typical behavior of OSEM and does not arise from a termination of contrast increasing but from noise increasing; the real behavior of OSEM is covered by the 3D Gauss filter and the number 80 is due to the filter, not to iterative reconstruction. The contrast at 80 iterations is higher in OSEM than in FBP for every level of lesion-to-background activity ratio, both with high and low background. The contrast gain using OSEM ranges from 6.7% to 16.4% for different C_{nom}.

The use of first order Chang's AC leads to diminished contrast values both in FBP and OSEM; again contrast values for OSEM-AC were higher than the ones obtained with FBP-AC. Kauppinen et al.[14] reported a contrast gain ranging from 7.1% to 12.5%, using a brain phantom with a gray-to-white matter activity ratio of 4:1, reconstructed with OSEM + variable 3D Gauss (72 iterations) and FBP (Butterworth: order 6, cutoff = 0.6 cm^{-1}), both with attenuation correction.

This situation is different when taking into account sphere contrast in "cold" lesions: contrast increases in OSEM reconstruction as iteration number increases, without reaching saturation. The equivalence between contrast in OSEM and FBP is reached at 80 iterations. Contrast values are dependent on background activity concentration, being smaller with high background. Moreover, the application of AC leads to a slight increase in contrast both with OSEM and FBP.

The tomographic spatial resolution with scatter expressed as axial, radial and tangential FWHM did not vary with increasing EM-equivalent iteration number. This finding was expected since resolution mainly depends on the collimator characteristics. The values obtained are significantly lower than the ones obtained with FBP with a high-resolution filter of clinical use. Also FBP with ramp filter shows FWHM values slightly higher than OSEM.

It must be acknowledged that conclusions are strongly affected by the adopted 3D Gauss filter of OSEM; a different filter would likely lead to other conclusions, at least from a quantitative point of view: without the 3D Gauss filter, OSEM optimization should be found more rapidly than after 80 iterations. Moreover OSEM should have better spatial resolution and contrast than FBP, both in hot and cold lesions, but with notable increase of noise with increasing EM-equivalent iteration number.

To devise the best performing image reconstruction algorithm with an optimal set of parameters in clinical use is an issue that cannot be addressed fully by the present work. First of all, this is because a geometric phantom is used that cannot reflect many of the subtle features of real clinical images. The analyses are based on computer measurements of quantities without interaction with human observers. Thus, the detailed quantitative results and conclusions are likely correct for the specific phantom imaging conditions, but the reader may wonder whether the conclusions are applicable to the real word of clinical images. Moreover, the problem of algorithm selection is intrinsically multi parametric and a simple recipe that holds for every situation cannot be devised. The optimal set of parameters depends on clinical task. For instance, if we are looking for hot lesions, then OSEM with the suggested threshold of 80 EM equivalent iteration and without AC correction will lead to an increase in contrast, a better spatial resolution and only a slight increase of noise that, in a study with a high count statistic, may be disregarded. On the other hand, if the study count statistic is low the increase of noise could be harmful and then we could better switch to FBP or OSEM with a smaller number of iterations to reach noise equivalence (for instance at 23 EM equivalent iterations in low background studies). In this case we still have better resolution with OSEM, but contrast for hot lesions will be worse than with FBP. If we are looking for cold lesions, the equivalence of contrast between OSEM and FBP is reached at 80 EM equivalent iterations, but noise is higher for OSEM than for FBP; the application of AC in this context will provide better contrast both for OSEM and FBP.

REFERENCES

1. Barret HH, Wilson DW, Tsui BMW. Noise properties of the EM algorithm: part I. Theory. *Phys Med Biol* 1994; 39: 833–846.
2. Liow J-S, Strother SC. Practical tradeoffs between noise, quantitation and number of iterations for maximum likelihood-based reconstruction. *IEEE Trans Med Imaging* 1991; 10: 563–571.
3. Miller TR, Wallis JW. Clinically important characteristics of maximum-likelihood reconstruction. *J Nucl Med* 1992; 33: 1678–1684.
4. Snyder DL, Miller MI, Thomas LJ Jr, Politte DG. Noise and edge artifacts in maximum likelihood reconstruction for emission tomography. *IEEE Trans Med Imaging* 1987; 6: 228–238.
5. Hudson HM, Larkin RS. Accelerated image reconstruction using ordered subsets of projection data. *IEEE Trans Med Imaging* 1994; 13: 601–609.
6. Yokoi T, Shinohara H, Onishi H. Performance evaluation of OSEM reconstruction algorithm incorporating three-dimensional distance-dependent resolution compensation for brain SPECT: a simulation study. *Ann Nucl Med* 2002; 16: 11–18.
7. Lau YH, Hutton BF, Beekman FJ. Choice of collimator for cardiac SPET when resolution compensation is included in iterative reconstruction. *Eur J Nucl Med* 2001; 28: 39–47.
8. Hutton BF, Baccarne V. Efficient scatter modelling for incorporation in maximum likelihood reconstruction. *Eur J*

Nucl Med 1998; 25: 1658–1665.
9. Hutton BF, Lau YH. Application of distance-dependent resolution compensation and post-reconstruction filtering for myocardial SPECT. *Phys Med Biol* 43: 1679–1693.
10. Kamphuis C, Beekman FJ, van Rijk PP, Viergever MA. Dual matrix ordered subsets reconstruction for accelerated 3D scatter compensation in single-photon emission tomography. *Eur J Nucl Med* 1998; 25: 8–18.
11. Lalush DS, Tsui BMW. Performance of ordered-subset reconstruction algorithms under conditions of extreme attenuation and truncation in myocardial SPECT. *J Nucl Med* 2000; 41: 737–744.
12. Blocklet D, Seret A, Popa N, Schoutens A. Maximum-likelihood reconstruction with ordered subsets in bone SPECT. *J Nucl Med* 1999; 40: 1978–1984.
13. Case JA, Licho R, King MA, Weaver JP. Bone SPECT of the spine: a comparison of attenuation correction techniques. *J Nucl Med* 1999; 40: 604–613.
14. Kauppinen T, Koskinen MO, Alenius S, Vanninen E, Kuikka JT. Improvement of brain perfusion SPET using iterative reconstruction with scatter and non-uniform attenuation correction. *Eur J Nucl Med* 2000; 27: 1380–1386.
15. Vanhove C, Defrise M, Franken PR, Everaert H, Deconinck F, Bossuyt A. Interest of the ordered subsets expectation maximization (OS-EM) algorithm in pinhole single-photon emission tomography reconstruction: a phantom study. *Eur J Nucl Med* 2000; 27: 140–146.
16. Wells GR, King MA, Simkin PH, Judy PF, Brill AB, Gifford HC, et al. Comparing filtered backprojection and ordered subsets expectation maximization for small-lesions detection and localization in ^{67}Ga SPECT. *J Nucl Med* 2000; 41: 1391–1399.
17. Gonzalez RC, Wood RE. *Digital Image Processing. Reading*, MA; Addison Wesley Publishing, 1992: 208–209.
18. Iftikar I, Koutelou M, Mahmarian JJ, Verani MS. Simultaneous perfusion tomography and radionuclide angiography during dobutamine stress. *J Nucl Med* 1996; 37: 1306–1310.
19. Kiat H, Maddhai J, Roy LT, et al. Comparison of technetium 99m methyl isobutyl isonitrile ant thallium 201 for evaluation of coronary artery disease by planar and tomographic methods. *Am Heart J* 1989; 117: 1–11.
20. Taillefer R, DePuey EG, Udelson JE, Bellar GA, Latour Y, Reeves F. Comparative diagnostic accuracy of Tl-201 and Tc-99m sestamibi SPECT imaging (perfusion and ECG-gated SPECT) in detecting coronary artery disease in women. *J Am Coll Cardiol* 1997; 29: 69–77.
21. Chang LT. A method for attenuation correction in radionuclide computed tomography. *IEEE Trans Nucl Sci* 1978; 25: 638–643.
22. Beekman FJ, Viergever MA. Evaluation of fully 3D iterative scatter compensation and post-reconstruction filtering in SPECT. In: Grangeat P, Amans J-L, eds. *Three-dimensional image reconstruction in radiology and nuclear medicine*. Dordrecht Boston London; Kluwer Academic Publishers, 1996: 163–175.
23. Pedroli G, Crespi A, De Agostini A, Farinelli C, Moretti R, et al. The quality control of SPET systems: results of an inter-laboratory comparison study in Italy. *J Nucl Med and All Sci* 1989; 33: 396–400.
24. Winer BJ. *Statistical principles in experimental design*. New York; McGraw-Hill, 1971.
25. Hutton BF, Hudson HM, Beekman FJ. A clinical perspective of accelerated statistical reconstruction. *Eur J Nucl Med* 1997; 24: 797–808.
26. Wallis JW, Miller TR. Rapidly converging iterative reconstruction algorithms in single-photon emission computed tomography. *J Nucl Med* 1993; 34: 1793–1800.